Electronic Supplementary Information

Magnetoimpedance spectroscopy of phase-separated $La_{0.5}Ca_{0.5}MnO_3$ polycrystalline manganites

Mourad Smari[a,b,*], Rihab Hamdi[b,c], Jesús Prado-Gonjal[d], Raquel Cortés-Gil[e], Essebti Dhahri[a], Federico Mompean[d], Mar García-Hernández[d], Rainer Schmidt[f,g*]

[a] *CICECO, Aveiro Institute of Materials, Department of Materials and Ceramic Engineering, University of Aveiro, 3810-193 Aveiro, Portugal*

[b] *Laboratory of Applied Physics, University of Sfax, B.P. 1171, Sfax 3000, Tunisia*

[c] *College of Health and Life Sciences, Hamad Bin Khalifa University, Qatar Foundation, Doha, Qatar*

[d] *Instituto de Ciencia de Materiales de Madrid ICMM-CSIC, Sor Juana Inés de la Cruz 3, 28049 Madrid, Spain*

[e] *Departamento de Química Inorgánica, Facultad de Ciencias Químicas, Universidad Complutense de Madrid, 28040 Madrid, Spain*

[f] *GFMC, Departamento de Física de Materiales, Facultad de Ciencias Físicas, Universidad Complutense de Madrid, 28040 Madrid, Spain*

[g] *Unidad Asociada "Laboratorio de heteroestructuras con aplicación en espintrónica", UCM/CSIC, 28049 Madrid, Spain*

*Corresponding authors: smarimourad97@gmail.com; rainerxschmidt@googlemail.com

ESI 1. Neutron diffraction study of $La_{0.5}Ca_{0.5}MnO_3$ at room temperature

Table ESI 1

Lattice parameter, a / Å	5.4158(2)
Lattice parameter, b / Å	7.6430(2)
Lattice parameter, c / Å	5.4247(2)
La / Ca (position 4c)	
x	0.0189(7)
z	-0.0013(9)
β_{11} x 10^4 / Å²	75(10)
β_{22} x 10^4 / Å²	29(5)
β_{33} x 10^4 / Å²	69(10)
Occ. La / Ca (0.25/0.25)	0.241(8) / 0.247(8)
Mn (position 4b)	
β_{11} x 10^4 / Å²	44(10)
β_{22} x 10^4 / Å²	10(5)
β_{33} x 10^4 / Å²	65(15)
Occ. Mn (0.5)	0.492(6)
O1 (position 4c)	
x	-0.008 (5)
z	0.4400(8)
β_{11} x 10^4 / Å²	135(20)
β_{22} x 10^4 / Å²	19(5)
β_{33} x 10^4 / Å²	90(10)
Occ. O (0.5)	0.5
O2 (position 8d)	
x	0.7236(6)
y	-0.0306(3)
z	0.2762(7)
β_{11} x 10^4 / Å²	73(9)
β_{22} x 10^4 / Å²	44(4)
β_{33} x 10^4 / Å²	117(10)
Occ. O2 (1)	1
R_p (%) / R_{wp} (%)	1.66 / 2.21
R_{exp} (%)	4.71
Bragg R-factor	1.54
***Pnma* (#62): 4c(x¼ z), 4b(0 0 ½), 8d(xyz)**	

ESI 2. X-ray thermodiffraction study of $La_{0.5}Ca_{0.5}MnO_3$

Table ESI 2

	Pnma				$P2_1/m$				Refinement agreement factors
T (K)	**a**	**b**	**c**	**b/√2**	**a**	**b**	**c**	**β**	
298	5.425(1)	7.642(1)	5.4189(9)	5.404					R_p: 5.48; R_{wp}:7.40; R_{exp}:6.46 χ^2: 1.31
270	5.422(1)	7.6408(9)	5.4192(9)	5.403					R_p: 6.06; R_{wp}:8.52; R_{exp}:6.02 χ^2: 2.01
250	5.4215(8)	7.632(1)	5.4131(9)	5.397					R_p: 5.96; R_{wp}:8.12; R_{exp}:6.10 χ^2: 1.77
230	5.420(1)	7.6233(9)	5.411(1)	5.390					R_p: 5.80; R_{wp}:8.02; R_{exp}:6.62 χ^2: 1.89
210	5.421(1)	7.6188(9)	5.414(1)	5.387					R_p: 5.40; R_{wp}:7.47; R_{exp}:6.14 χ^2: 1.48
190	5.420(1)	7.618(1)	5.4147(9)	5.387					R_p: 7.13; R_{wp}:9.68; R_{exp}:6.66 χ^2: 2.11
170	5.418(1)	7.592(1)	5.400(1)	5.369					R_p: 5.98; R_{wp}:8.19; R_{exp}:6.17 χ^2: 1.76
150	5.4179(9)	7.596(2)	5.401(1)	5.371	5.4546(3)	10.8651(8)	7.5292(6)	90.097(2)	R_p: 4.64; R_{wp}:6.27; R_{exp}:6.18 χ^2: 1.03
130	5.416(1)	7.609(2)	5.402(1)	5.381	5.462(1)	10.8730(9)	7.5209(6)	90.039(2)	R_p: 4.69; R_{wp}:6.40; R_{exp}:6.17 χ^2: 1.08
110	5.416(1)	7.617(2)	5.401(1)	5.387	5.4635(8)	10.8749(7)	7.5191(6)	90.042(1)	R_p: 4.73; R_{wp}:6.40; R_{exp}:6.18 χ^2: 1.07
90	5.416(1)	7.6191(8)	5.401(9)	5.387	5.4641(3)	10.8751(4)	7.5189(4)	90.038(4)	R_p: 4.75; R_{wp}:6.43; R_{exp}:6.13 χ^2: 1.10
70	5.4158(9)	7.619(2)	5.4002(1)	5.387	5.4636(4)	10.8735(9)	7.5181(4)	90.038(5)	R_p: 4.84; R_{wp}:6.60; R_{exp}:6.12 χ^2: 1.16
15	5.418(1)	7.623(2)	5.394(1)	5.391	5.4614(3)	10.8701(6)	7.5163(4)	90.100(5)	R_p: 4.98; R_{wp}:6.63; R_{exp}:6.18 χ^2: 1.15

Figures ESI 2 X-ray diffraction patterns for $La_{0.5}Ca_{0.5}MnO_3$ powder at different temperatures. Observed intensities are printed in red dots, Rietveld refined curves are printed as full black lines, and the difference between the two by blue lines underneath. The expected Bragg reflections are marked by blue and red dashes for *Pnma* and $P2_1/m$ phases respectively.

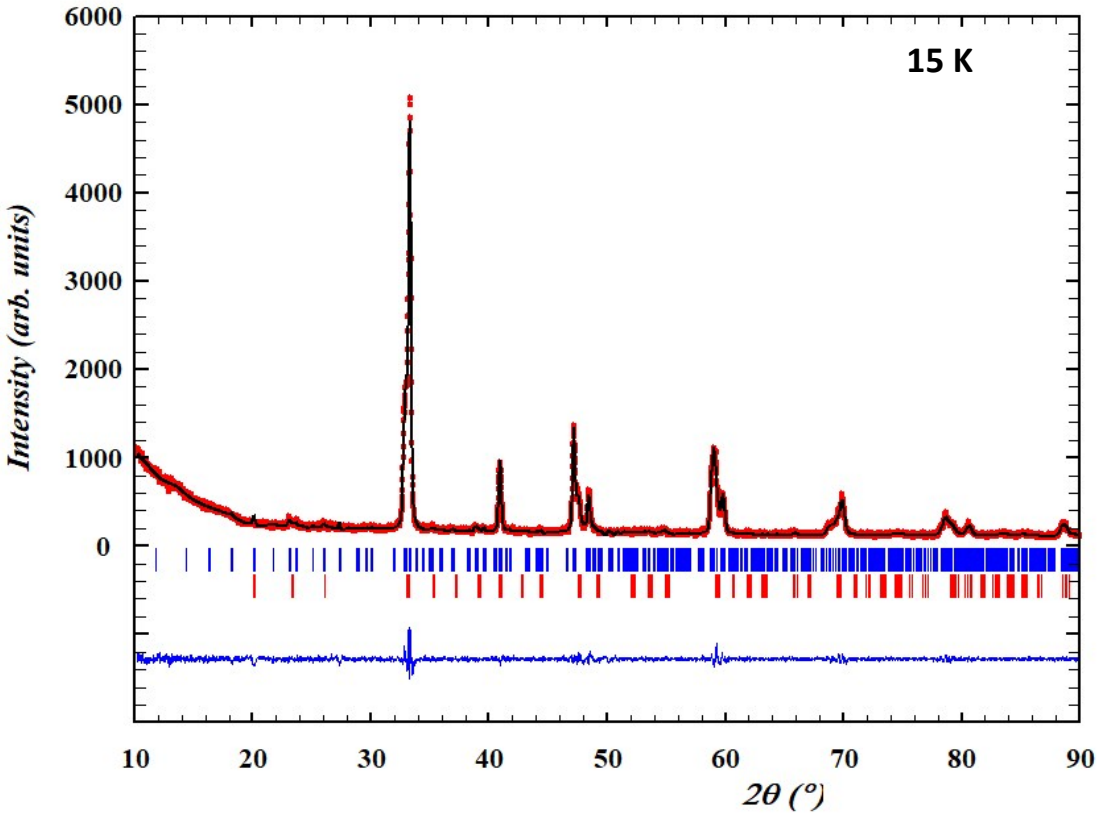
15 K
Intensity (arb. units)
6000
5000
4000
3000
2000
1000
0
10
20
30
40
50
60
70
80
90
2θ (°)

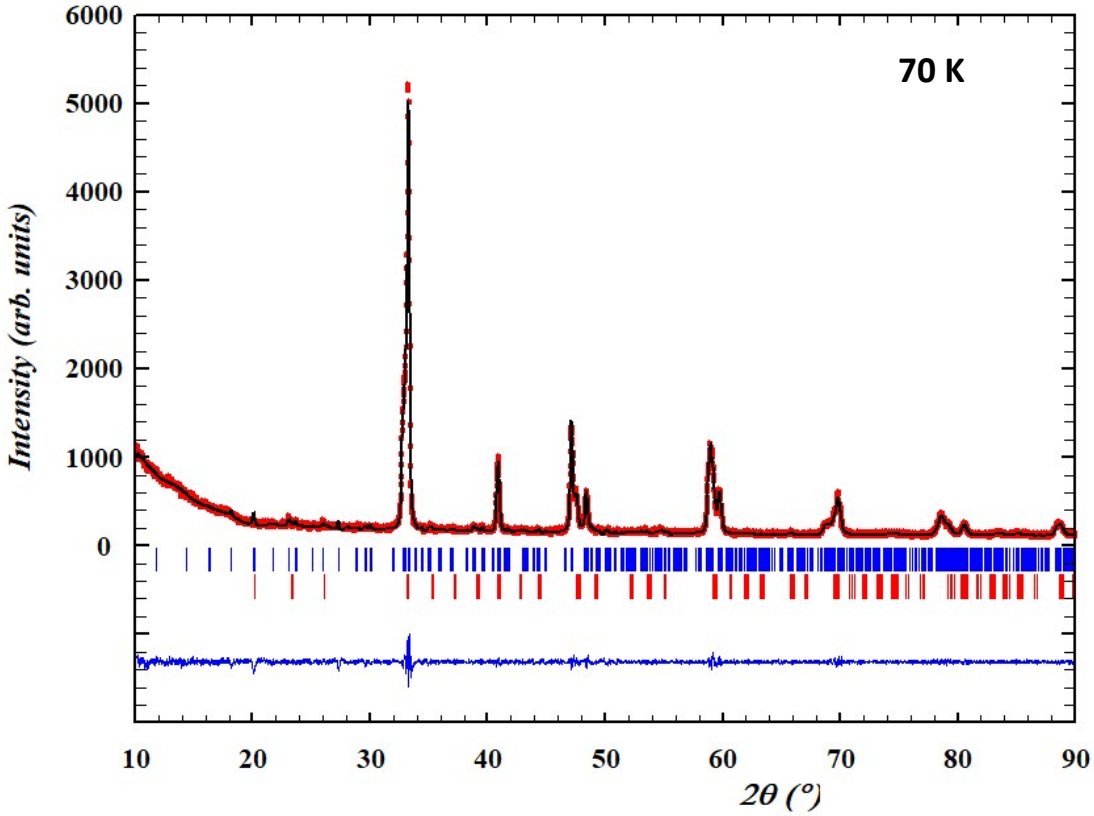
70 K
Intensity (arb. units)
6000
5000
4000
3000
2000
1000
0
10
20
30
40
50
60
70
80
90
2θ (°)

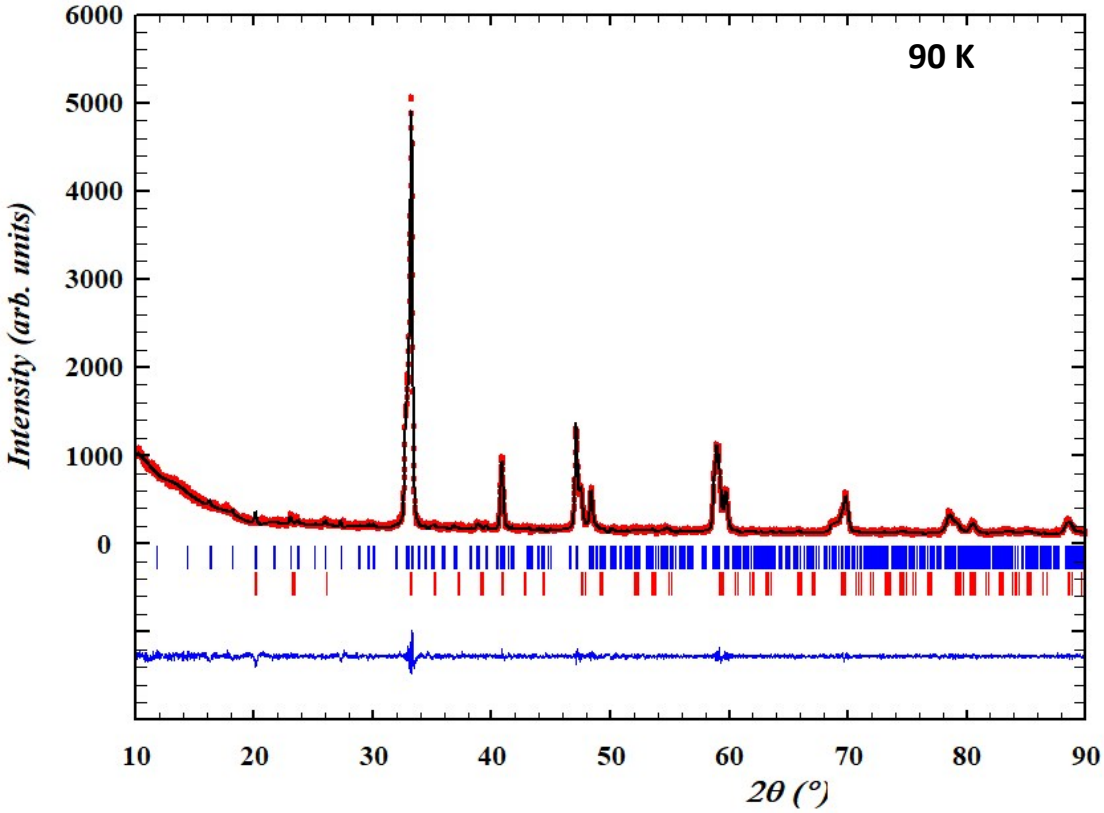
90 K
Intensity (arb. units)
6000
5000
4000
3000
2000
1000
0
10
20
30
40
50
60
70
80
90
2θ (°)

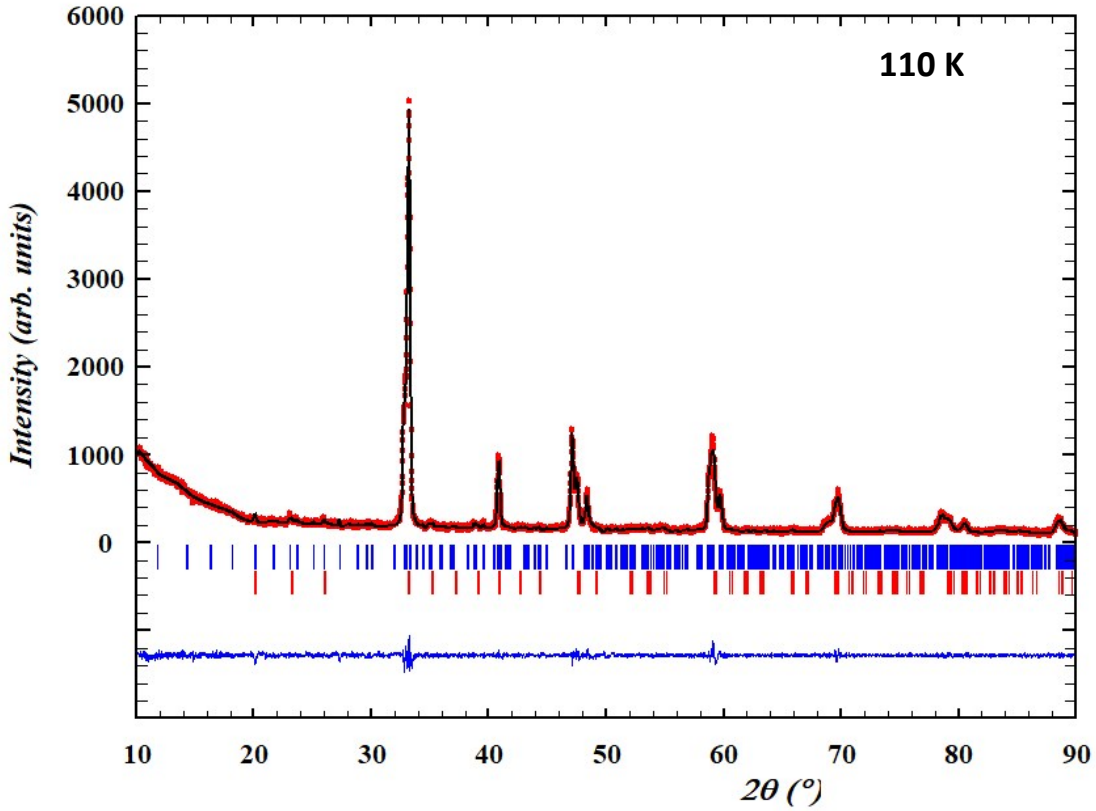
110 K
Intensity (arb. units)
6000
5000
4000
3000
2000
1000
0
10
20
30
40
50
60
70
80
90
2θ (°)

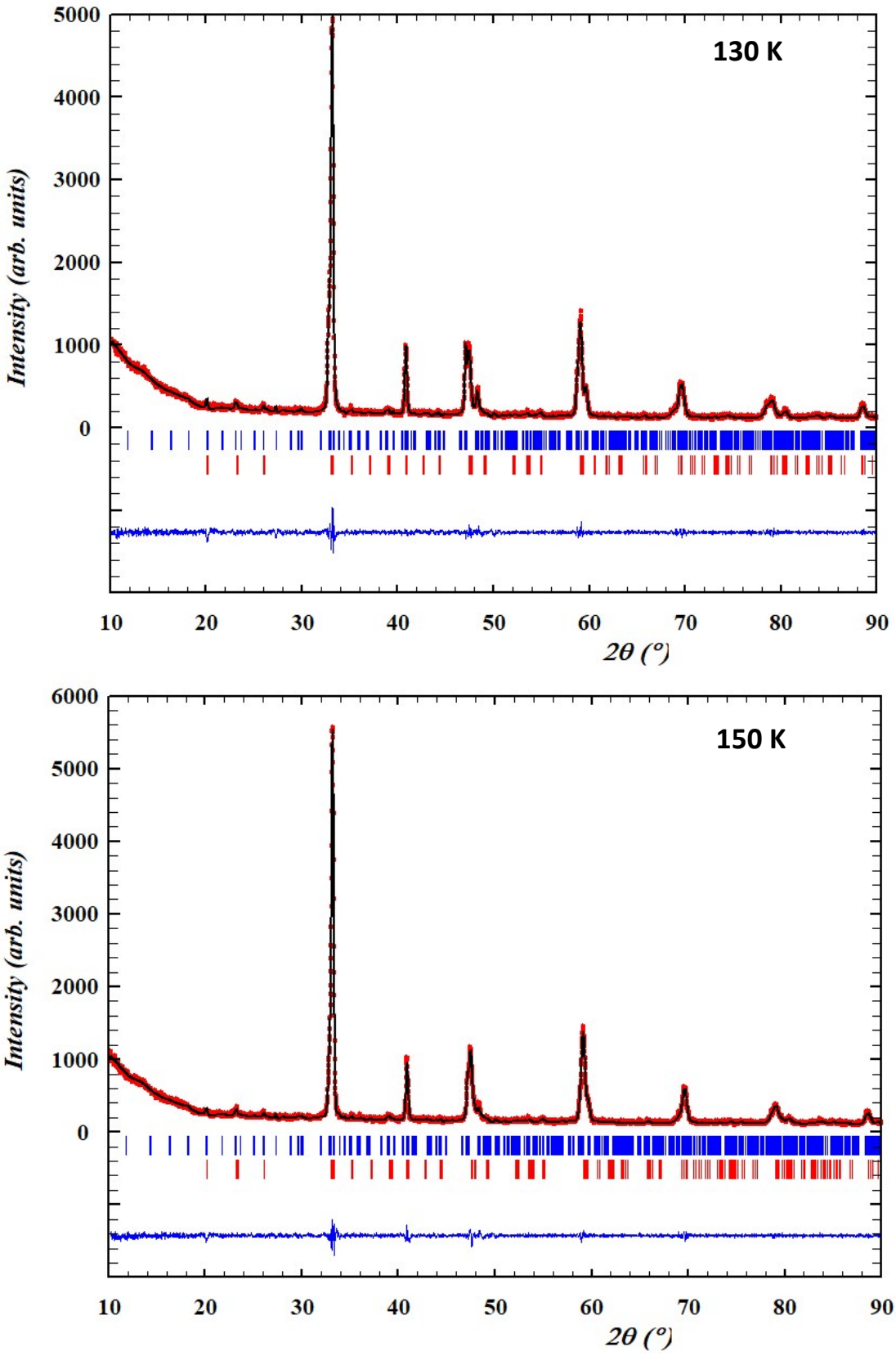
130 K
150 K
Intensity (arb. units)
2θ (°)
0
1000
2000
3000
4000
5000
6000
10
20
30
40
50
60
70
80
90

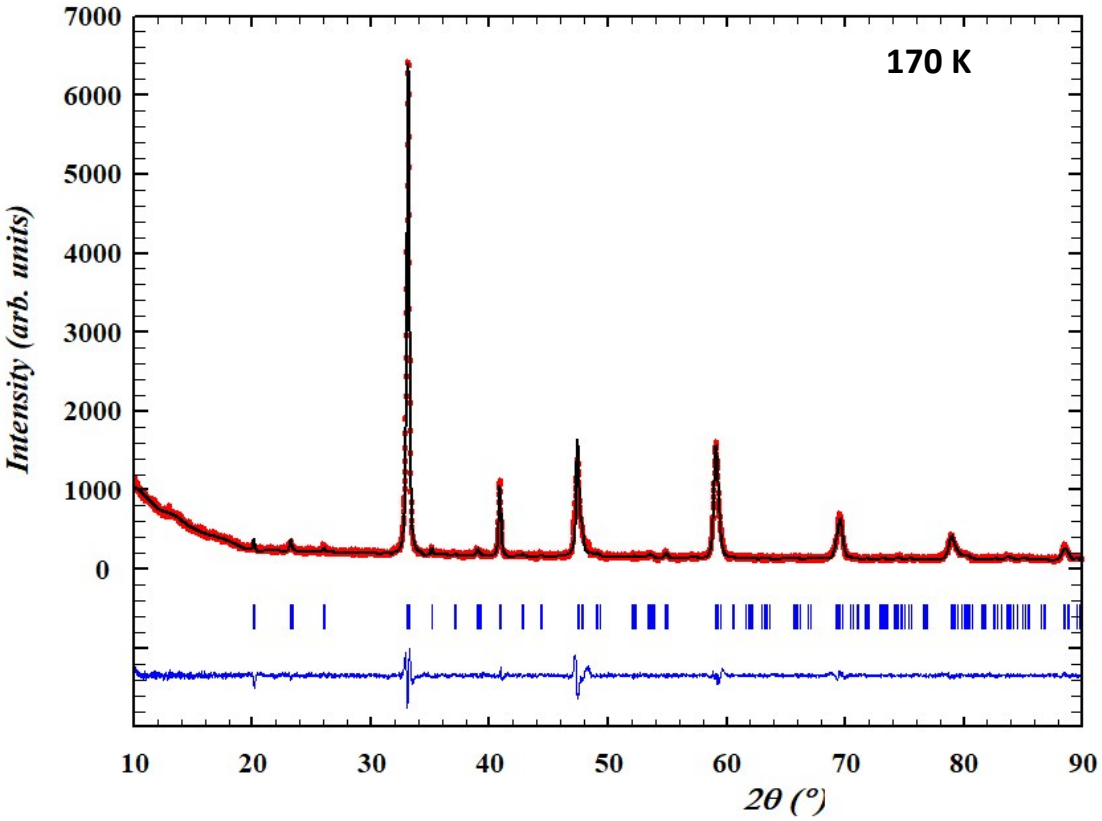
170 K
Intensity (arb. units)
7000
6000
5000
4000
3000
2000
1000
0
10
20
30
40
50
60
70
80
90
2θ (°)

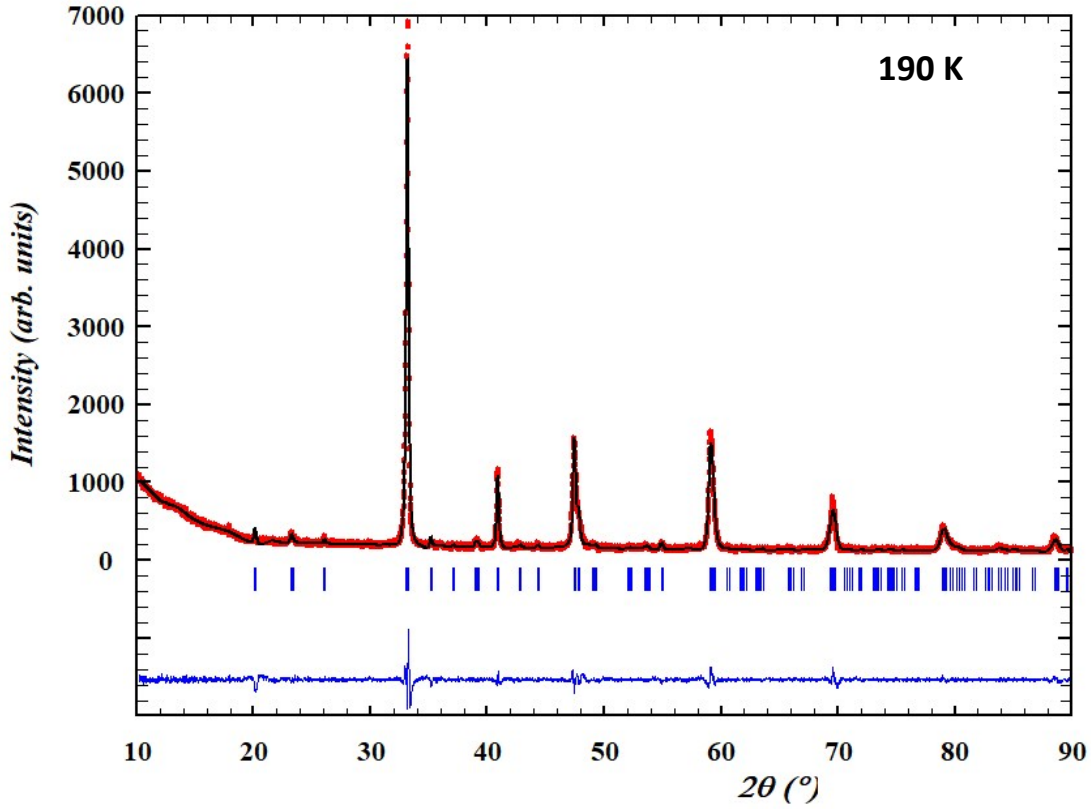
190 K
Intensity (arb. units)
7000
6000
5000
4000
3000
2000
1000
0
10
20
30
40
50
60
70
80
90
2θ (°)

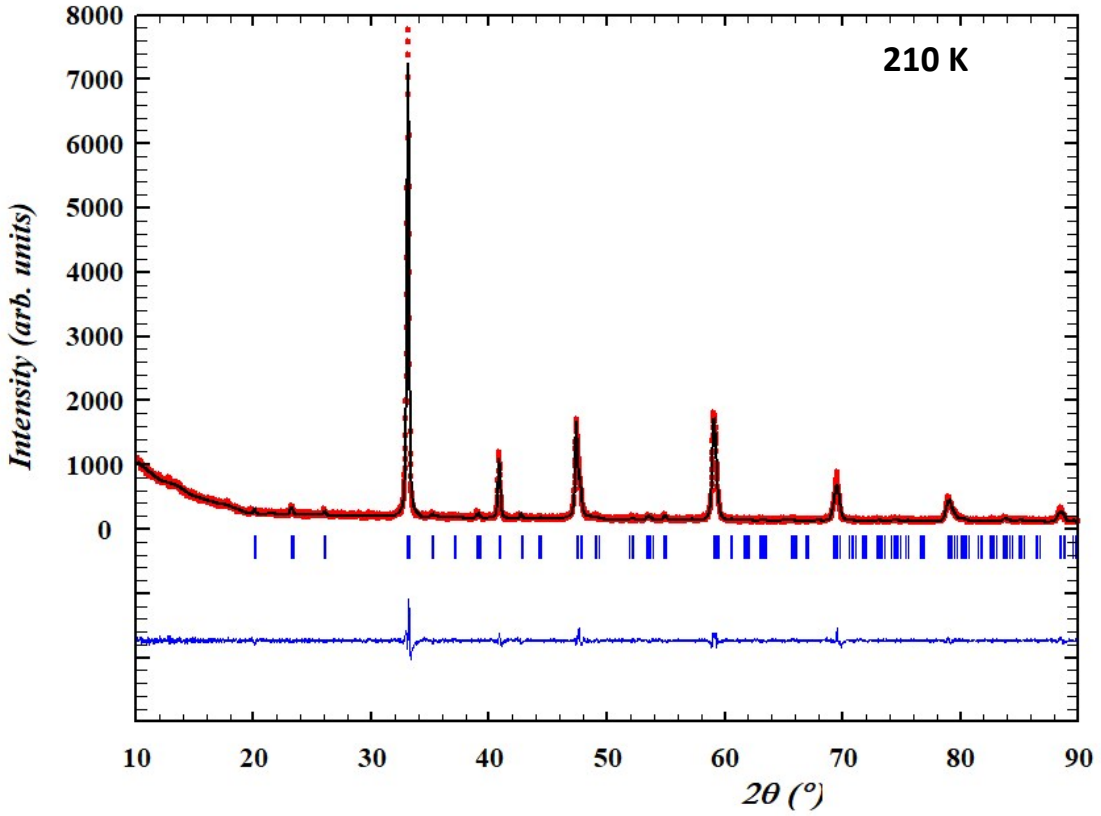
210 K
Intensity (arb. units)
2θ (°)

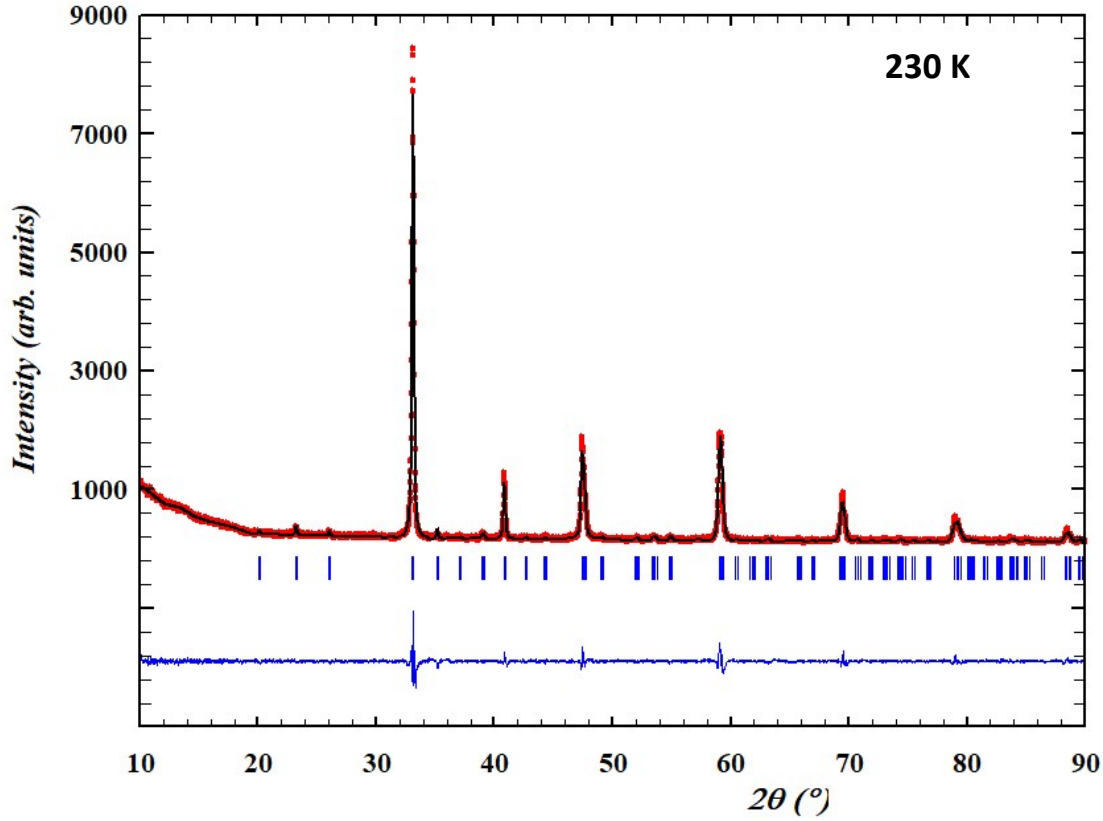
230 K
Intensity (arb. units)
2θ (°)

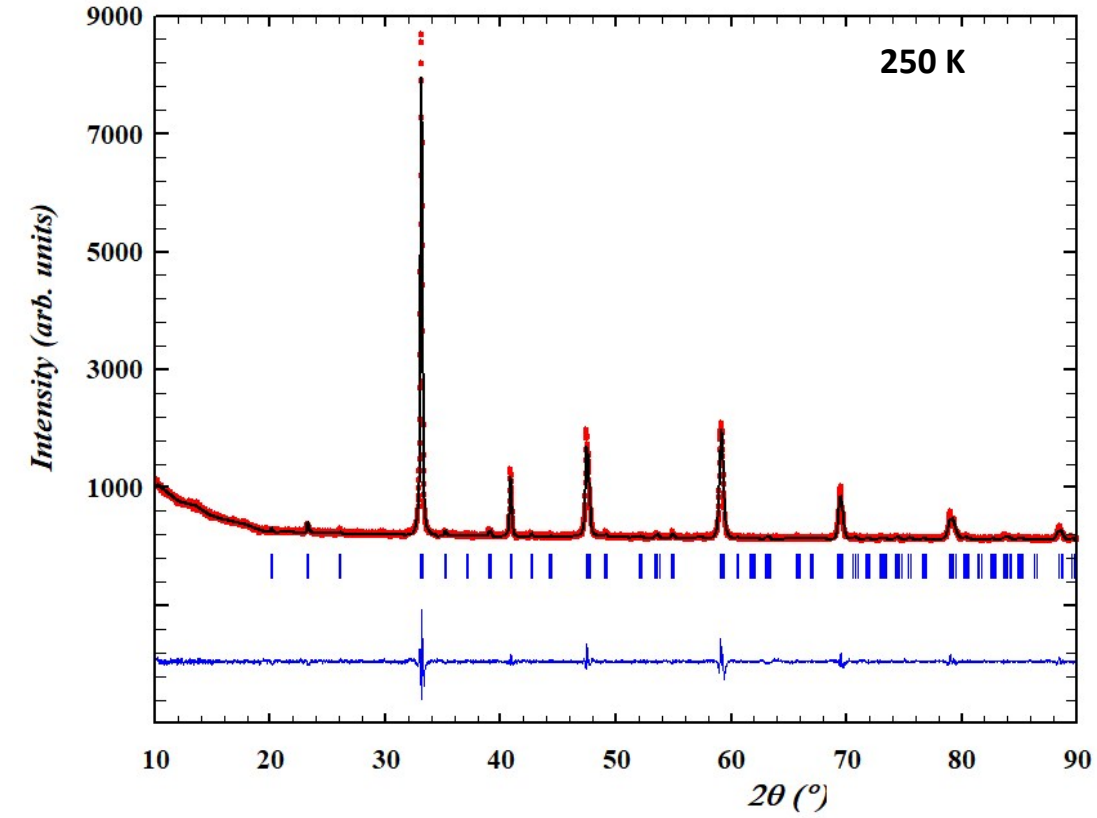
250 K
Intensity (arb. units)
9000
7000
5000
3000
1000
10
20
30
40
50
60
70
80
90
2θ (°)

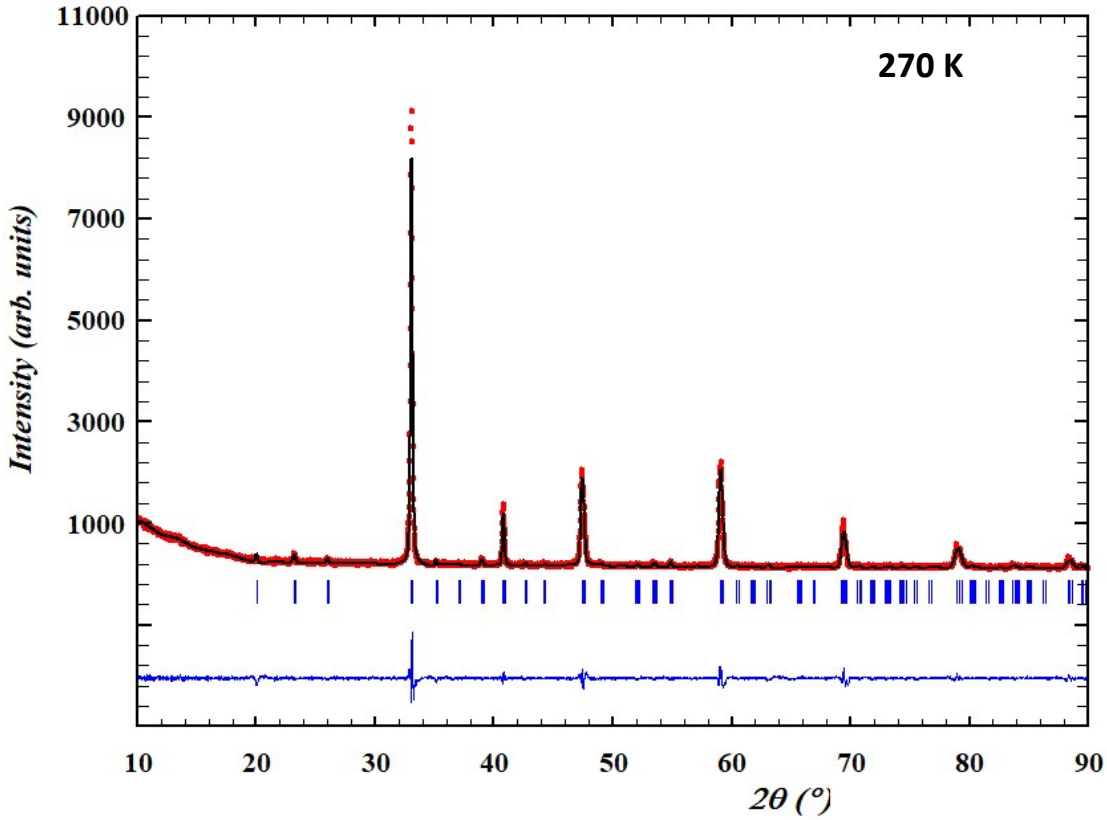
270 K
Intensity (arb. units)
11000
9000
7000
5000
3000
1000
10
20
30
40
50
60
70
80
90
2θ (°)

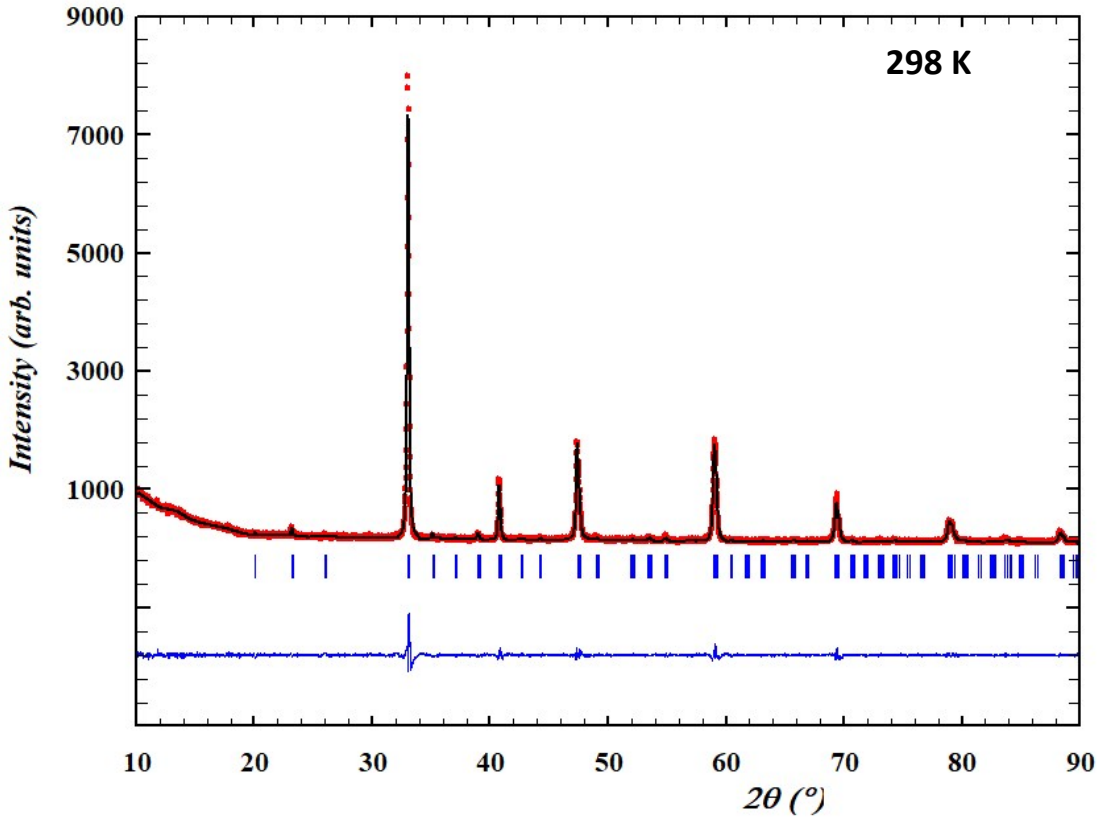
298 K
Intensity (arb. units)
9000
7000
5000
3000
1000
10
20
30
40
50
60
70
80
90
2θ (°)

ESI 3. *M* vs *H* curves for $La_{0.5}Ca_{0.5}MnO_3$ powder between 5 K and 300 K

Figures ESI 3 *M* vs *H* curves for $La_{0.5}Ca_{0.5}MnO_3$ powder between 5 K - 300 K and 0 - 14 T.

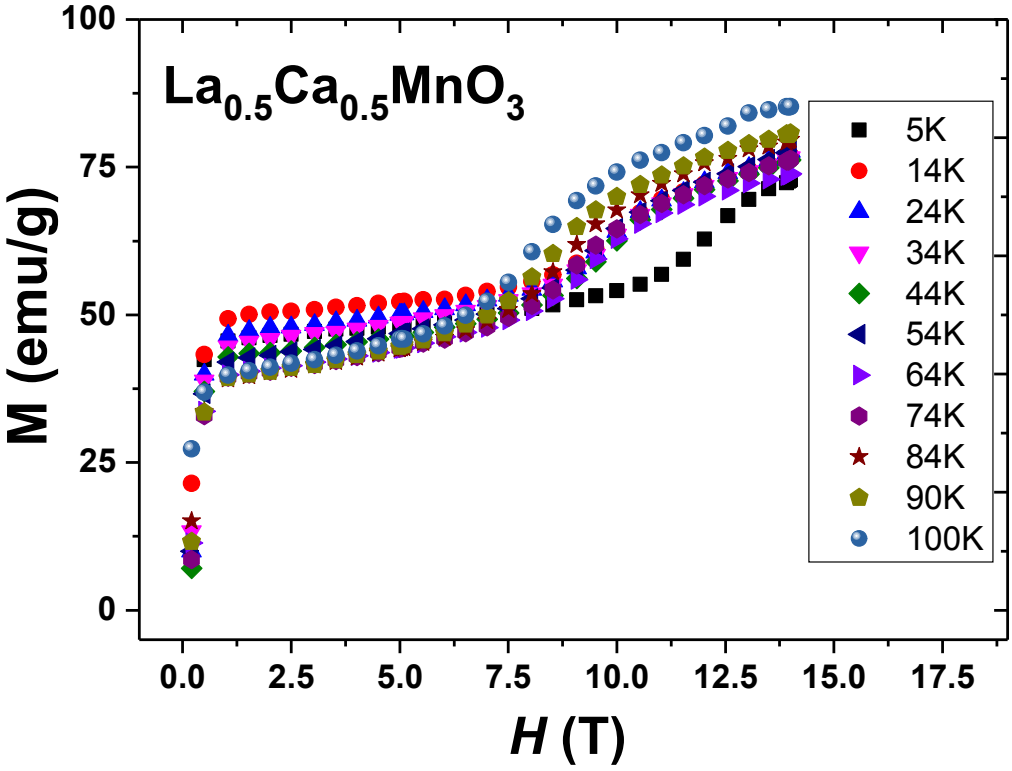

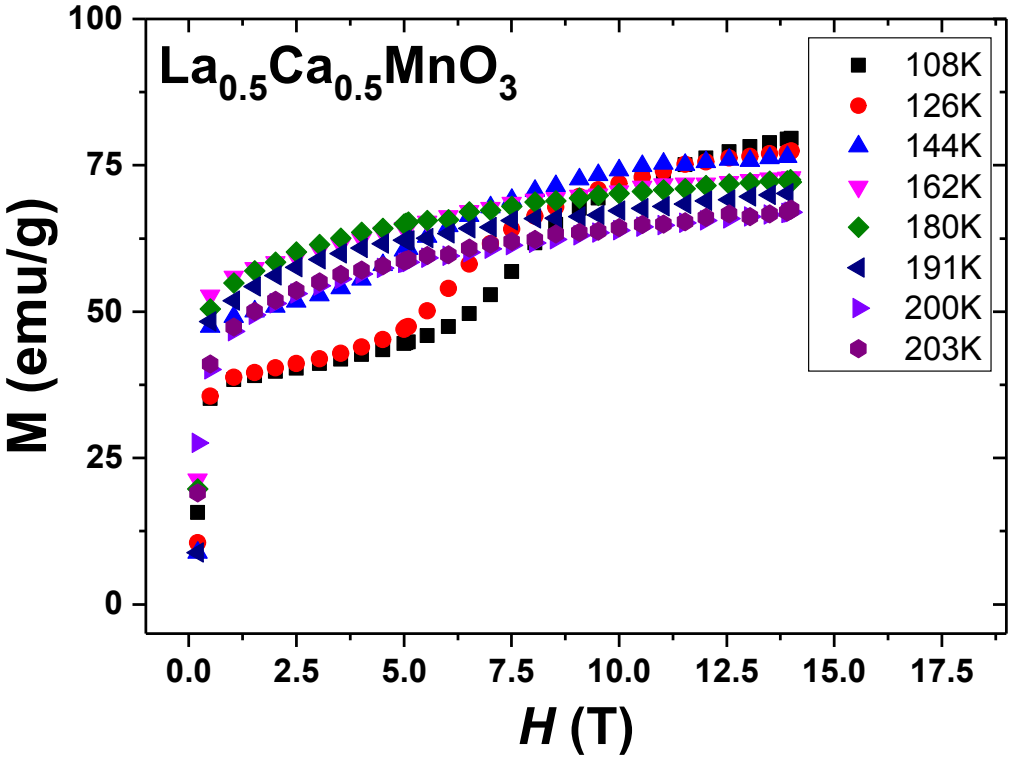

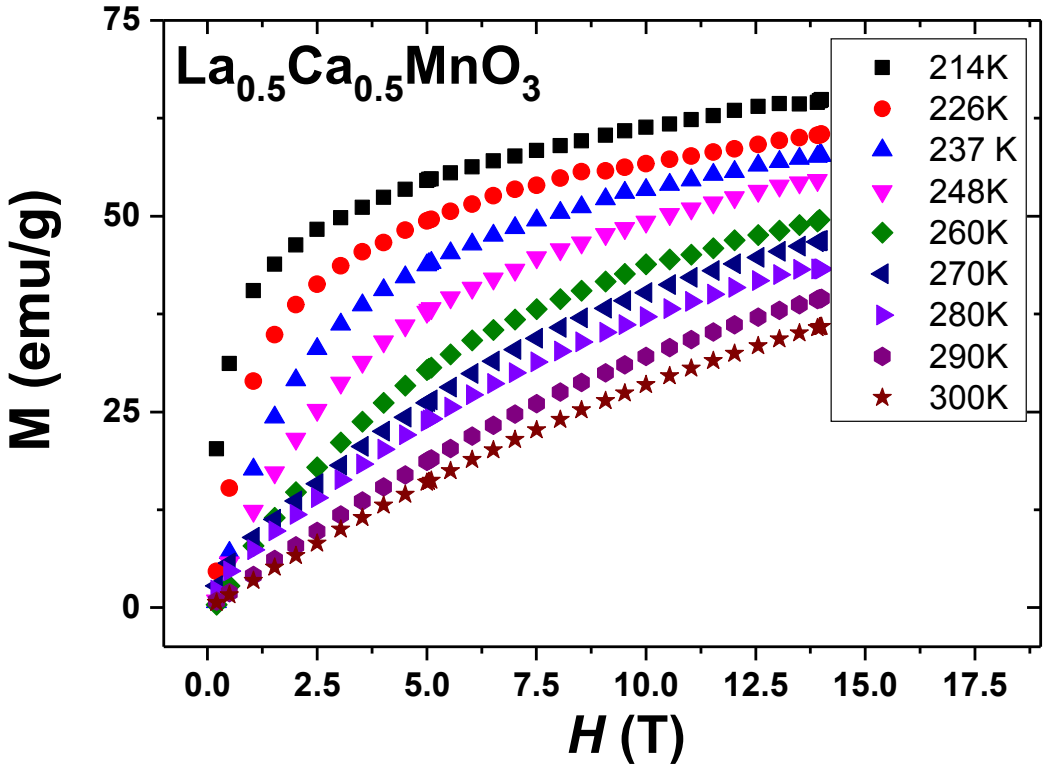
La0.5Ca0.5MnO3
214K
226K
237 K
248K
260K
270K
280K
290K
300K
M (emu/g)
H (T)
75
50
25
0
0.0
2.5
5.0
7.5
10.0
12.5
15.0
17.5

ESI 4. Basic principles of impedance spectroscopy

Impedance spectroscopy is a well-established tool for the separate analysis of several dielectric contributions to the macroscopic dielectric properties of solid matter [1-3]. Impedance spectroscopy experiments consist in the application of an electric stimulus in terms of a time (t)-dependent alternating voltage signal U of variable angular frequency ω ($\omega = 2\pi f$) and fixed amplitude U_0 applied to the sample under test: $U(\omega, t) = \boldsymbol{U_0} \sin(\boldsymbol{\omega} t)$ (see Figure ESI 3, blue arrow).

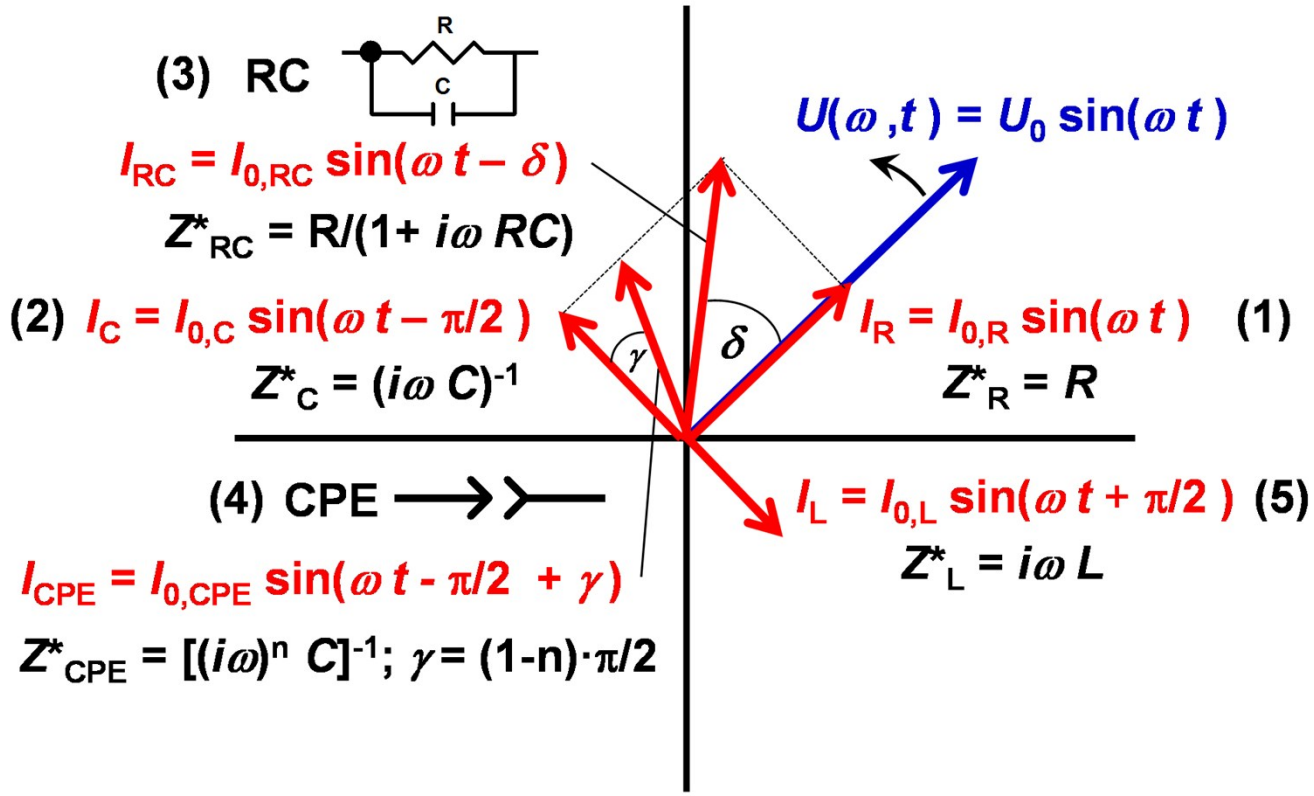

Figure ESI 3 Phasor diagram for an applied voltage signal U (blue arrow) and the current response (red arrows) of an (1) ideal resistor (I_R), (2) ideal capacitor (I_C), (3) ideal RC element (I_{RC}), (4) non-ideal constant phase element (I_{CPE}), and (5) ideal inductor (I_L). The complex impedance for the equivalent circuit components R, C, RC, CPE and L are given. The current response of different components is characterised by the amplitude (length of the red arrows) and a characteristic phase shift.

Effectively, the impedance spectroscopy apparatus measures the amplitude I_0 and phase shift δ of the alternating current response signal I (Figure ESI 3, red arrows for different possible current response signals) over a wide frequency range: $I(\omega, t) = I_0 \sin(\omega t + \delta)$. One period of the applied voltage signal corresponds to a 2π (360°) rotation of the $U(\omega,t)$ arrow on the phasor diagram shown in Figure ESI 3. For the most common equivalent circuit elements the current response is (1) in phase ($\delta = 0$) with the applied voltage for an ideal resistor, I_R, (2) out of phase by $\delta = -\pi/2$ for an ideal capacitor, I_C, (3) out of phase by an f-dependent phase shift $0 < \delta < -\pi/2$ for an ideal parallel resistor-capacitor (RC) element, (4) out of phase by $\delta = -\pi/2 + \gamma$ for a constant-phase element (CPE) that can be regarded a "non-ideal" capacitor, and (5) out of phase by $\delta = +\pi/2$ for an ideal inductor, I_L. Note that CPEs displays an f-independent phase shift γ, thus the name constant phase element, where the angle γ is accounted for with respect to an ideal capacitor. The angle γ is correlated to the critical CPE exponent n (see Figure ESI 3), which in turn is correlated with the degree of suppression of the typical semicircle arc below the real x-axis in complex impedance plane plots of Z'' vs Z' (Figures 5a and 6a in the main text).

All phase angles are t- independent, which implies that all arrows in Figure ESI 3 would rotate at the same ω with t-independent phase angles. This illustrates that the impedance can be defined as a t-independent complex number, $Z^* = Z' + iZ''$. The impedance fraction in phase with $U(\omega,t)$ is defined as the real, and the part out of phase by +/- $\pi/2$ as the positive/negative imaginary part. By definition, a negative phase shift corresponds to a current preceding the applied voltage U as is the case for an ideal capacitor (I_C), which leads to a negative imaginary part of impedance Z'', whereas a positive phase shift corresponds to a current lagging behind U as is the case for an ideal inductor (I_L) and leads to positive Z''.

In practice, impedance spectra of insulating or semiconducting samples show predominantly negative Z'', but a crossover from negative (capacitive) to positive (inductive) Z'' at high ω can sometimes

occur in more conducting samples. Note that the impedance for an inductor (Z^*_L) increases linearly with ω or f, whereas the impedance of a capacitor (Z^*_C) decreases with the proportionality ~$1/\omega$ or ~ $1/f$ (see Figure ESI 3). This implies that inductive contributions would appear in the impedance spectra at sufficiently high-f. In the case that an inductive contribution may be dominant over a certain high-f regime, it is not possible to extract the capacitance of the relevant dielectric contribution. Z'' is positive and the capacitance is thus not accessible. The opposite applies in capacitive lower f regimes, where only the capacitance of the respective dielectric contribution may be determined but not the inductance. The equivalent circuits applied to impedance spectroscopy data usually reflect that fact and are, thus made up of conventional RC elements to represent the f-ranges where capacitive contributions dominate, whereas for inductive dominated high-f ranges, they may contain inductive L-elements.

For the more common capacitive impedance response ($Z'' < 0$), each dielectric contribution in an insulating or semiconducting sample can usually be represented by an RC element. One RC element is visible in Z'' vs Z' complex impedance plane plots in form of one impedance semicircle arc. The arc diameter corresponds to R and the frequency where the arc has its maximum is given by $\omega_{max} = 1/RC = \tau^{-1}$. Each dielectric contribution (RC element) in the impedance response may be associated with a certain area in the sample like grain interior bulk or GBs, and the overall equivalent circuit model is then made up of a series connection of the various RC elements.

The RC element model can be understood intuitively. The application of a voltage stimulus to a sample leads to two instant and concurrent responses from that sample, i.e. dielectric polarization of localized charges and the concomitant displacement currents, as represented by the capacitor, and charge transport of mobile charge carriers and concomitant conduction currents, as represented by the resistor. Considering the example of an RC element representing an insulating material, the capacitor describes the polarizability of the material and its ability to store charge, and the parallel

resistor describes the sample's leakage resistance that arises from the charge transport of mobile charge carriers that bypass or "escape" the ideal charge storage element.

Almost all dielectric contributions encountered in experimental impedance spectra are usually not ideal as represented by ideal RC circuit elements, in which case ideal capacitors are commonly replaced by non-ideal CPEs. The true capacitance C of a dielectric contribution, as represented by a possible R-CPE element, and the critical CPE exponent n can be extracted using equivalent circuit fitting software [4], where $n = 1$ for an ideal capacitor, $n < 1$ measures the non-ideality of the dielectric contribution and $n > 1$ is unphysical. As mentioned above, the critical exponent n from the CPE is correlated with the degree of suppression of the semicircle arc in plots of Z'' vs Z', which indicates the width of the distribution of dielectric relaxation times τ. The CPE is usually interpreted as a sign for a certain distribution of τ across the respective sample area, where $\tau = \mathrm{R} \times \mathrm{C} = \rho\, \varepsilon_0\, \varepsilon_r'$ in an ideal RC element and decreasing n indicates an increasing width of the distribution of τ. The exact shape of the distribution function of τ is not accessible from impedance spectroscopy data, since the CPE only yields one more additional parameter n, which is related to γ, and any attempt to determine the precise distribution function from impedance spectroscopy data should be regarded unphysical [5].

References

[1] E. Barsukov and J. Macdonald, *Impedance Spectroscopy: Theory, Experiment and Applications* (John Wiley & Sons Inc., Hoboken, 2005).

[2] R. Schmidt, in *Ceramic Materials Research Trends*, edited by P. B. Lin (Novascience Publishers, Hauppauge, 2007), p. 321.

[3] R. Schmidt, J. Wu, C. Leighton, and I. Terry, Phys. Rev. B **79**, 125105 (2009).

[4] C. H. Hsu and F. Mansfeld, Corrosion **57**, 747 (2001).

[5] R. Schmidt, W. Eerenstein, T. Winiecki, F. D. Morrison, and P. A. Midgley, Phys. Rev. B **75**, 245111 (2007).

ESI 4. Equivalent circuit fits

A data file (ESI 4. Equivalent circuit fits.xlsx) is attached to this publication, which contains all fitted parameters as extracted from the fitting software. The resistance and capacitance values are not normalized, i.e. given in Ω and Farad.